UPGRADE OF THE SPS ION INJECTION SYSTEM

J. Uythoven, J. Borburgh, E. Bravin, S. Burger, E. Carlier, J.-M. Cravero, L. Ducimetière, S. Gilardoni, B. Goddard, J. Hansen, E.B. Holzer, M. Hourican, T. Kramer, F. Maciariello, D. Manglunki, F.-X. Nuiry, A. Perillo Marcone, G. Steele, F. Velotti, H. Vincke, CERN, Geneva, Switzerland

Abstract

As part of the LHC Injectors Upgrade Project (LIU) the injection system into the SPS will be upgraded for the use with ions. The changes will include the addition of a Pulse Forming Line parallel to the existing PFN to power the kicker magnets MKP-S. With the PFL a reduced magnetic field rise time of 100 ns should be reached. The missing deflection strength will be given by two new septum magnets MSI-V, to be installed between the existing septum MSI and the kickers MKP-S. A dedicated ion dump will be installed downstream of the injection elements. The parameter lists of the elements and studies concerning emittance blow-up coming from the injection system are presented. The feasibility of the 100 ns kicker rise time and the small ripple of the septum power converter are presented. Material studies of the ion dump are presented together with the radiation impact.

INTRODUCTION

The ALICE experiment in the LHC will be implementing a detector upgrade to reach higher luminosities with ion operation. The foreseen ALICE peak luminosity in Pb-Pb runs is 7×10^{27} Hz/cm^2. As part of the LHC Injector Upgrade Project (LIU), an upgrade of the LHC ion injection chain is ongoing to reach this ambitious goal [1]. The LIU ion project consists of upgrades throughout the ion injector complex and also of the injection system for the ions in the SPS, see Fig. 1.

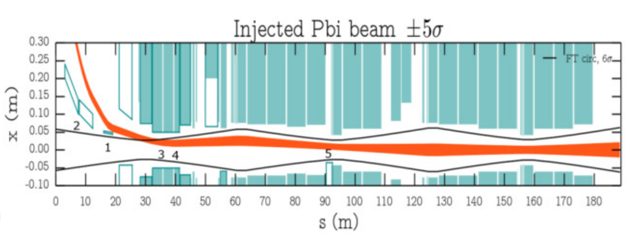

Figure 1: Trajectory and 5σ envelope of the injected ion beam together with the proposed layout: the new MSI-V septum (1), the existing septum MSI (2), the fast injection kickers MKP-S (3) and the slower injection kicker MKP-L (4) together with the new ion injection dump (5).

The new injection system for ions will allow a spacing of 100 ns between the ions batches in the SPS, due to an upgrade of the SPS injection kicker MKP, obtaining a faster pulse rise time. The resulting reduced kick strength will be compensated by the installation of an additional septum MSI-V. As the trajectory of the injected beam is different from the one of the protons, a new injection dump for ions will be installed. A new beam observation screen will be placed in front of the dump and additional beam loss monitors will be added. Details of some of the new or modified elements will be given below.

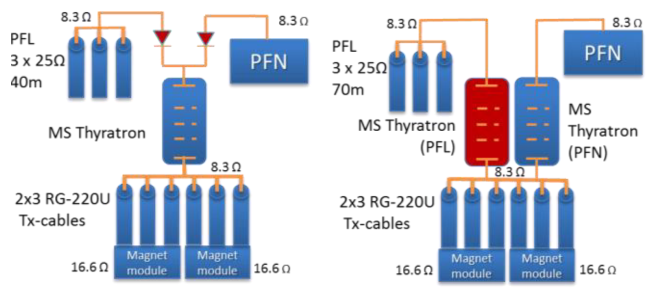

Figure 2: MKP 100 ns test set-up: Configuration 1with diode for separation between PFL and PFN (left) and configuration 2 with one thyratron per branch (right).

INJECTION KICKER UPGRADE

The upgrade of the existing SPS ion injection system by adding an additional PFL in parallel to the existing MKP-S PFN generators is outlined in [2]. In order to proof the feasibility of the 100 ns rise time (2-98%) and to validate the preliminary PSpice simulations a test stand for the 100 ns MKP-S upgrade was set up. Two basic options for a low impedance connection of the existing PFN to the PFL and the transmission cables, as shown in Fig. 2, were developed. Whilst configuration 1 considers only one main switch (MS) thyratron connected to the six parallel transmission cables (50 Ω RG-220U, 3 per magnet module) and separated for operation by two diode stacks, the same functionality is obtained in configuration 2 by using a 2nd thyratron for the PFL branch.

Measurements with the test system in configuration 1 have been performed and showed a significant increase of rise time due to the additional diode stack in the PFL branch. Rise times of around 350 ns were measured with a first test setup using switch tank connected to the spare MKP-S magnet via short transmission cables. Whilst optimization of the circuits (filters) would bring large improvements, it will not stay below the specified 100 ns rise time.

Activities will now focus on tests for configuration 2 which however requires mechanical modification on both switch tanks. Also more detailed PSpice simulations will be necessary to optimize the filter circuits mainly to

ISBN 978-3-95450-168-7

reduce flat top ripple whilst keeping the fast rise time. The measurements also suggest that pulse steepening ferrites might be necessary to mitigate the pre-pulse ripples currently outside the 2% threshold.

Table 1: Injection Elements with Deflection and Ripple

Element	Nominal deflection	Ripple
MSI	42.8 mrad	100 ppm
MSI-V	12.3 mrad	500 ppm
MKP	2.069 mrad	± 1 %

BEAM BLOW-UP DUE TO RIPPLE

The contribution to the emittance growth in case of unmatched beam trajectory has been estimated for the three injection elements MSI, MIS-V and MKP using the analytical formula for emittance blow-up [3]. The assumed deflection and ripple are given in Table 1. The results of the calculations are summarised in Fig. 3. For an MSI-V ripple of 500 ppm, the contribution to the emittance blow-up will be similar to the MSI contribution. The total is dominated by the injection kicker ripple and for injection kicker ripple above ± 1 % the transverse damper system is required to keep the emittance blow-up within specification.

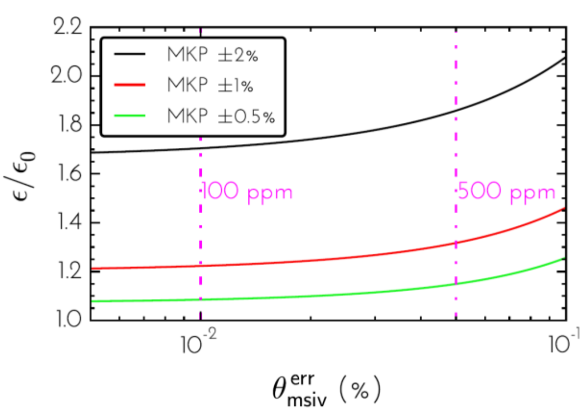

Figure 3: Expected total emittance blow-up as a function of MSI-V current ripple, without transverse damper.

SPS ION DUMP

The design of a new SPS injection ion dump is guided by several restrictions. Firstly the space available is limited meaning the total length of the device must be in the region of 1 m, including any vacuum flanges if required. Secondly the device should be robust enough to not need replacing during the remaining operational lifetime of the accelerator, and should survive all foreseen ion beams. Thirdly it must adequately protect the surrounding area in terms of radiation to other devices and any nearby access areas.

FLUKA [4, 5] simulations were performed for a variety of materials considering the beam dimensions given in Table 2. For all cases the beam considered was Pb^{82+} with an equivalent energy of 17.1 GeV/proton, which corresponds to a $^{208}Pb^{82+}$ kinetic energy of 5.9 GeV/u. To ensure simulations are conservative a bunch intensity of 3.8 x 10^8 ions was assumed with the possibility of 4 bunches per shot.

Table 2: Beam Dimensions at Dump

Emittance [um]	Spot size horizontal [mm]	Spot size vertical [mm]
Normal – 1.3	0.40	0.80
Mid – 1.0	0.35	0.70
Tight – 0.5	0.25	0.50

Transient thermal simulations using ANSYS [6], considering a cooling pipe (diameter: 15mm) along the full length of the dump water cooled with a forced convection coefficient of 1000 W/(m^{2}K), show that the steady state condition is reached after few (about 10) consecutive pulses.

Transient structural simulations were performed over a total time of 1 µs, in order to simulate mechanical stresses not only during the pulse time (0.304 µs) but also the effect of the thermal shock waves after the impact.

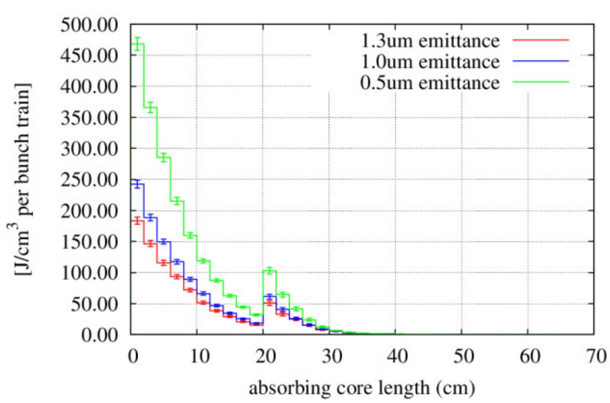

Figure 4: Peak energy density for an ion injection dump in 0.2 m of Be plus 0.5 m of Cu, for 3 different emittance beams.

The restricted space available for the device leads to a preference for a material which does not need baking out, avoiding the need for extra vacuum equipment. Both copper and aluminium were considered for use as the beam absorber but rejected due to seeing stresses above the safe limits. The most promising metallic option considered was beryllium. Since the peak energy deposition occurs very near the front face of the absorber, a sandwich structure was proposed with 0.2 m of beryllium followed by 0.5 m of copper, to reduce the cost of the device and to increase the protection offered to downstream objects. There is a significant increase in the peak energy density seen in a material with the smallest emittance beams (see Fig 4). For the beryllium this increase results in stresses above the acceptable material limits in case impacted by the tightest beam. The results

ISBN 978-3-95450-168-7

summarised in Table 3 show that a combination of 0.2 m beryllium followed by 0.5 m of copper would be able to withstand the middle and the normal emittance beam.

Another, more “exotic” option, was to consider Quarzal® (type N) as first material of the combination, keeping copper for the second part of the dump; in this case simulations show that the dump would withstand even the tightest emittance beam. However, further investigations on the properties of Quarzal® need to be made before selecting the material.

Table 3: Summary of the maximum thermo-mechanical stresses for the different options considered. The last two columns give the ratio of tensile and compressive stresses calculated and the assumed material limit.

Material	Ex,y [μm]	T-max [°C]	Tensile ratio	Compr. ratio
Be in Be-Cu	0.5	144	57/345	-394/-207
Cu in Be-Cu	0.5	47	17/250	-87/-250
Be in Be-Cu	1.0	88	31/345	-182/-207
Cu in Be-Cu	1.0	37	14/250	-56/-250
Qu in Qu-Cu	0.5	296	0.4/8	-2/-65
Cu in Qu-Cu	0.5	79	43/250	-199/-250
Bn in Bn-Cu	0.5	265	1.5/46	-7/-10
Cu in Bn-Cu	0.5	57	25/250	-121/-250
Gr in Gr-Cu	0.5	299	2/30	-12/-118
Cu in Gr-Cu	0.5	54	27/250	-125/-250

The materials considered for the first 0.2 m of the dump block that could also survive the small emittance beams are in general prone to outgassing, thus increasing the complexity of the design. Options considered, of which the results are also listed in Table 2, are graphite and hot pressed boron nitride, both of which have been used extensively elsewhere at CERN. The graphite-copper option is the preferred from a stress calculation point of view, seen the resulting safety margins.

Further fatigue analysis will need to be done on the selected material, taking into account the cycles that the ion dump can see during its life time.

DUMP ENCLOSURE

Simulations show that for the presented combination of low-Z material followed by copper, the copper part needs to be shielded. In the case of a dump assumed entirely out of copper, a 20 cm marble shielding leads to a dose rate reduction of about a factor of 10, see Fig. 5. At a lateral distance of 40 cm to the dump one finds a residual dose rate of 4 mSv/h, without shielding.

With 20 cm of marble shielding, only at the extremities of the dump one still finds high dose rate levels which can be explained by the direct, unshielded view on the highly activated copper. As a consequence of that, the copper part of the sandwich (low-Z material followed by copper) should be shielded laterally and at its extremities by 20 cm of marble.

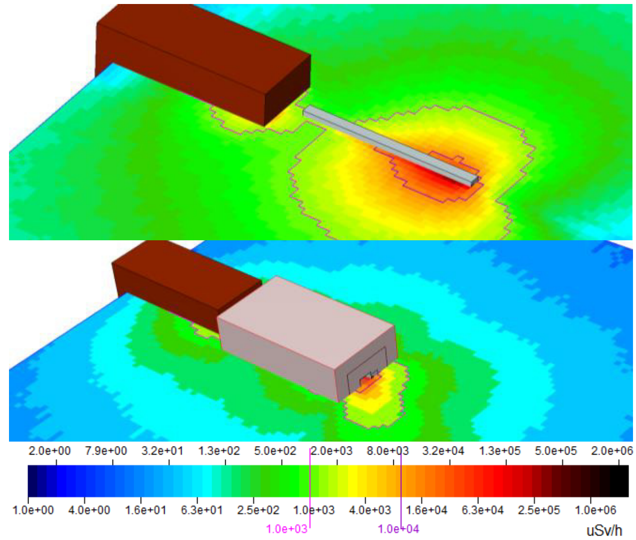

Figure 5: Residual dose rate in the vicinity of a copper beam dump under worst case ion beam dump operation (3.5E13 $^{208}Pb^{82+}$ ions at 5.9 GeV/u kinetic energy being dumped within one day) followed by a cool down period of 1 day. The upper picture show the radiation levels without, the lower with marble shielding.

CONCLUSIONS

Several studies on the new SPS injection channel have been carried out. Simulations and first experimental test of the injection kicker powered by an additional PFL show that it is not possible to obtain the specified 100 ns rise time and most likely the system will need to operate with two thyratrons in parallel, one for the PFN and one for the PFL. The emittance growth at injection is also dominated by the kicker ripple and a ripple of 500 ppm on the new septum MSI-V seems acceptable.

To be effective, the new ion dump will need to consist of a sandwich of a low Z followed by a high Z material. The choice of the low Z material depends on the assumed transverse emittance of the ion beam, as very low emittances can lead to unacceptable compressive stresses. An additional marble shielding of the dump can significantly reduce the residual dose rate.

REFERENCES

[1] M.Bodendorfer et al., ‘Ions: Baseline studies plan and strategy for the pending options’, LHC performance workshop, Chamonix, 22 – 25 September 2014.
[2] T. Kramer, et al., “Upgrade of the SPS Injection Kicker System for LHC High Luminosity Operation with Heavy Ion Beam”, proc. IPAC14, Dresden, 2014.
[3] A. Wu Chao, M.Tigner, “Handbook of Accelerator Physics Engineering”, 2006.
[4] T.T. Bohlen et al., "The FLUKA Code: Developments and Challenges for High Energy and Medical Applications", Nuclear Data Sheets 120, 211-214 (2014).

[5] A. Ferrari, P.R. Sala, A. Fasso`, and J. Ranft "FLUKA: a multi-particle transport code", CERN-2005-10 (2005), INFN/TC_05/11, SLAC-R-773.

[6] ANSYS® Academic Research, Release 15.0.

ISBN 978-3-95450-168-7